

Fusion cross-section for Ni-based reactions within the relativistic mean field formalism

M. Bhuyan^{1*} and Raj Kumar^{2†}

¹*Instituto Tecnológico de Aeronáutica, 12.228-900 São José dos Campos, São Paulo, Brazil*

²*School of Physics and Materials Science, Thapar Institute of Engineering and Technology, Patiala-147004, Punjab, India*

(Dated: May 26, 2022)

In this theoretical study, we establish an interrelationship between the nucleon-nucleon interaction potential and the nuclear fusion reaction cross-sections at low energies. The axially deformed self-consistent relativistic mean field with non-linear NL3* force is used to calculate the density distribution of the projectile and target nuclei for fusion. The Wong formula is used to estimate the fusion cross-section and barrier distribution from the nucleus-nucleus optical potential for Ni-based systems, which are known for fusion hindrance phenomena. The results of the application of the so obtained nucleus-nucleus optical potential for the fusion cross-section from the recently developed relativistic NN -interaction (R3Y) are compared with the well-known, phenomenological M3Y effective NN potential. We found a relatively good results from R3Y interactions below the barrier energies as compare to the M3Y potential concerning the experimental data. We also observe the density dependence on the nuclear interaction potential in terms of nucleon-nucleon optical potentials.

PACS numbers: 21.65.Mn, 26.60.Kp, 21.65.Cd

I. INTRODUCTION

Efforts have been devoted to determining the nature of the nucleon-nucleon interaction since 1932, the discovery of the neutron by Chadwick as the heart of nucleus in nuclear physics [1–3]. In the simplest expression, the nucleon-nucleon (NN) interaction is considered as central and to have a typical square-well, Gaussian or Yukawa potential of various ranges and strengths, which can obtain the observed phase shifts in elastic-scattering processes [1, 4, 5]. The traditional goal of nuclear physics is to understand properties of atomic nuclei regarding the bare interaction between a pair of nucleons. Though substantial progress has taken place to understand it in some theoretical and experimental attempts, remains an open problem at present. A large number of interactions have been constructed via studying NN scattering, but there exist extensive modifications in the scattering behavior due to the presence of surrounding nucleons in a nucleus [4, 6–9]. Further, the reconstruction of NN - potential through particle exchanges is made possible by the development of quantum field theory [10–13]. An effective phenomenological interaction has an appropriate form to study the nuclear structure and dynamics, which typically depend on the local density of nucleus.

At low energy, one can assume that the interaction potential between a pair of nucleons is instantaneous and therefore the concept of a substantial theory of nuclear forces, applicable to nuclear structure calculations [14–17]. The analytical derivation of potential through particle exchange is important to understand the nuclear force as well as structural properties via the nucleus-nucleus optical potential for the study of many nuclear aspects

such as nuclear radioactivity, nuclear scattering, nuclear fission and fusion process [18–20]. More fundamental approach to NN -interactions at low energies has been formulated by Refs [14, 17, 21–23] in terms of an effective theory for non-relativistic nucleons. It involves a few basic coupling constants, which have been determined from nucleon scattering data at low energies. Furthermore, the new effective NN -interaction entitled R3Y potential [18–20] analogous to the M3Y form [3] can be derived from the relativistic mean field Lagrangian. This interaction depends on the relativistic force parameters, the coupling constant among the interacting mesons and their masses [18–20]. One can see various potentials in more details and use them in future studies for some general and up-to-date views on the subject, look, for instance in Refs. [11–13, 21, 22]. Further, the nucleus-nucleus optical potential is quite important in the studies of elastic scattering of light and heavy-ion (HI) systems, in particular for the simple one-dimensional barrier penetration model (BPM) of fusion reaction, the barrier energy, the radius, and curvature via nuclear potential and Coulomb potential [24–26]. A microscopic description is required for calculating the interaction potential that incorporate the physical process, which can significantly influences the fusion process. The widely used methods to obtain the nuclear potential by integrating an NN -interaction over the matter distributions of the two colliding nuclei and the approach is called the double folding model [24–26]. It produces the nucleus-nucleus optical potential for further use in various studies including the radioactive decays [18–20, 27–29].

At low energy, the system can fuse either by penetrating the interaction barrier or it must have sufficient energy to overcome Coulomb barrier to get absorb. In the present study, we have considered the Ni-based reactions i.e $^{64}\text{Ni} + ^{64}\text{Ni}$, $^{64}\text{Ni} + ^{124}\text{Sn}$, $^{64}\text{Ni} + ^{132}\text{Sn}$, $^{58}\text{Ni} + ^{58}\text{Ni}$, $^{58}\text{Ni} + ^{124}\text{Sn}$, and $^{58}\text{Ni} + ^{132}\text{Sn}$ as their

* Email: bhuyan@ita.br

† Email: rajkumar@thapar.edu

fusion excitation functions are available experimentally and also known for fusion hindrance [30–39]. Below the Coulomb barrier, the nuclear structure effects dominate the resulting fusion dynamics, whereas the centrifugal potential suppresses the structure effects at above barrier energies. The estimation of fusion characteristics of heavy ions at extreme sub-barrier energies are of great interest for understanding the reaction mechanisms in astrophysics and the synthesis of the superheavy nuclei [40–42]. Hence, it is one of the great interest at present to see the performance of relativistic R3Y potential along with the microscopic relativistic mean field density to estimating the nuclear interaction potential for the study of fusion reaction at low energies. The present calculations are limited to the spherical coordinate system to generate the nucleus-nucleus interaction potential. One may consider the coupling between fusion and other degrees of freedom to generate a multidimensional potential barrier, which enhanced the fusion probabilities [40–45]. More detail studies of the multidimensional fusion barrier and their effect on the fusion dynamics can find from the Refs. [30–52].

This paper is organized as follows: In Sec. II we discuss the theoretical model for the relativistic mean field approach along with double folding procedure to get microscopic nucleus-nucleus optical potential. The Wong formula is also discussed in this section to study the fusion characteristics. Sec. III is assigned to the discussion of the results obtained from our calculation and of the possible correlation among the NN potential and fusion cross-section. Finally, a summary and a brief conclusion are given in Sec. IV.

II. RELATIVISTIC MEAN-FIELD FORMALISM

At present, the quantum chromodynamics (QCD) is not conceivable to describe the complete picture of the hadronic matter due to its non-perturbative properties. Hence, one needs to apply the perspective of effective field theory (EFT) at low energy, known as quantum hadrodynamics (QHD) [53–55]. The mean field treatment of QHD has been used widely to describe the nuclear structure and infinite nuclear matter characteristics [53–63]. In the relativistic mean field approach, the nucleus is considered as a composite system of nucleons interacting through exchange of mesons and photons [54, 64–68]. Here, most of the computational effort is devoted to solving the Dirac equation and to calculate various densities. We have used the microscopic self-consistent relativistic mean field (RMF) theory as a standard tool to investigate fusion study via Wong formula. The form of a typical relativistic Lagrangian density for a nucleon-meson

many body system, [53, 54, 58–72]

$$\mathcal{L} = \bar{\psi} \{ i\gamma^\mu \partial_\mu - M \} \psi + \frac{1}{2} \partial^\mu \sigma \partial_\mu \sigma - \frac{1}{2} m_\sigma^2 \sigma^2 - \frac{1}{3} g_2 \sigma^3 - \frac{1}{4} g_3 \sigma^4 - g_s \bar{\psi} \psi \sigma - \frac{1}{4} \Omega^{\mu\nu} \Omega_{\mu\nu} + \frac{1}{2} m_\omega^2 \omega^\mu \omega_\mu - g_w \bar{\psi} \gamma^\mu \psi \omega_\mu - \frac{1}{4} \vec{B}^{\mu\nu} \cdot \vec{B}_{\mu\nu} + \frac{1}{2} m_\rho^2 \vec{\rho}^\mu \cdot \vec{\rho}_\mu - g_\rho \bar{\psi} \gamma^\mu \vec{\tau} \psi \cdot \vec{\rho}^\mu - \frac{1}{4} F^{\mu\nu} F_{\mu\nu} - e \bar{\psi} \gamma^\mu \frac{(1 - \tau_3)}{2} \psi A_\mu. \quad (1)$$

The ψ are the Dirac spinors for the nucleons. The isospin and the third component of the iso-spin are denoted by τ and τ_3 , respectively. Here g_σ , g_ω , g_ρ and $\frac{e^2}{4\pi}$ are the coupling constants for σ –, ω –, ρ – meson and photon, respectively. The constant g_2 and g_3 are for the self-interacting non-linear σ –meson field. The masses of the σ –, ω –, ρ – mesons and nucleons are m_σ , m_ω , m_ρ , and M , respectively. The quantity A_μ stands for the electromagnetic field. The vector field tensors for the ω^μ , $\vec{\rho}_\mu$ and photon are given by,

$$F^{\mu\nu} = \partial_\mu A_\nu - \partial_\nu A_\mu \quad (2)$$

$$\Omega_{\mu\nu} = \partial_\mu \omega_\nu - \partial_\nu \omega_\mu \quad (3)$$

and

$$\vec{B}^{\mu\nu} = \partial_\mu \vec{\rho}_\nu - \partial_\nu \vec{\rho}_\mu, \quad (4)$$

respectively. From the above Lagrangian density we obtain the field equations for the Dirac nucleons and the mesons (i.e., σ , ω , and ρ , field) as,

$$\begin{aligned} (-i\alpha \cdot \nabla + \beta(M + g_\sigma \sigma) + g_\omega \omega + g_\rho \tau_3 \rho_3 + g_\delta \delta \tau) \psi &= e \psi, \\ (-\nabla^2 + m_\sigma^2) \sigma(r) &= -g_\sigma \rho_s(r) - g_2 \sigma^2(r) - g_3 \sigma^3(r), \\ (-\nabla^2 + m_\omega^2) V(r) &= g_\omega \rho(r), \\ (-\nabla^2 + m_\rho^2) \rho(r) &= g_\rho \rho_3(r). \end{aligned} \quad (5)$$

In the limit of one-meson exchange, for static baryonic medium, the solution of single nucleon-nucleon potential for scalar (σ), and vector (ω , ρ) fields are given by,

$$\begin{aligned} V_\sigma &= -\frac{g_\sigma^2}{4\pi} \frac{e^{-m_\sigma r}}{r} + \frac{g_2^2}{4\pi} \frac{e^{-2m_\sigma r}}{r^2} + \frac{g_3^2}{4\pi} \frac{e^{-3m_\sigma r}}{r^3} \\ \text{and} \\ V_\omega(r) &= +\frac{g_\omega^2}{4\pi} \frac{e^{-m_\omega r}}{r}, \quad V_\rho(r) = +\frac{g_\rho^2}{4\pi} \frac{e^{-m_\rho r}}{r}. \end{aligned} \quad (6)$$

The total effective NN –interaction is obtained from the scalar and vector parts of the meson fields. The recently developed relativistic NN –interaction potential analogous to M3Y form [3] entitled R3Y- potential. Here the R3Y potential is derived for the NL3* force, which is able to predict the nuclear matter as well as the properties of the finite nuclei at very high isospin asymmetries [18–20, 56, 57, 60, 61, 73, 74]. The relativistic effective

nucleon-nucleon interaction (V_{eff}^{R3Y}) for NL3* force along with the single-nucleon exchange effects as [3, 18–20, 57],

$$V_{eff}^{R3Y}(r) = \frac{g_\omega^2}{4\pi} \frac{e^{-m_\omega r}}{r} + \frac{g_\rho^2}{4\pi} \frac{e^{-m_\rho r}}{r} - \frac{g_\sigma^2}{4\pi} \frac{e^{-m_\sigma r}}{r} + \frac{g_2^2}{4\pi} \frac{e^{-2m_\sigma r}}{r^2} + \frac{g_3^2}{4\pi} \frac{e^{-3m_\sigma r}}{r^3} + J_{00}(E)\delta(s) \quad (7)$$

On the other hand, the M3Y effective interaction, obtained from a fit of the G-matrix elements based on Reid-Elliott soft-core NN -interaction [3], in an oscillator basis, is the sum of three Yukawa's (M3Y) with ranges 0.25 fm for a medium-range attractive part, 0.4 fm for a short-range repulsive part and 1.414 fm to ensure a long-range tail of the one-pion exchange potential (OPEP). The widely used M3Y effective interaction ($V_{eff}^{M3Y}(r)$) is given by

$$V_{eff}^{M3Y}(r) = 7999 \frac{e^{-4r}}{4r} - 2134 \frac{e^{-2.5r}}{2.5r}, \quad (8)$$

where the ranges are in fm and the strength in MeV. Note that Eq. (8) represents the spin- and isospin-independent parts of the central component of the effective NN -interaction, and that the OPEP contribution is absent here. Comparing Eqs. (7) and/or (8), we find similarity in the behavior of the NN -interaction and feel that Eq. (7) can be used to obtain the nucleus-nucleus optical potential. One can find more details in the Refs. [18, 19, 57]. The nuclear interaction potential, $V_n(R)$, between the projectile (p) and the target (t) nuclei, with the respective RMF (NL3*) calculated nuclear densities ρ_p and ρ_t , is

$$V_n(\vec{R}) = \int \rho_p(\vec{r}_p) \rho_t(\vec{r}_t) V_{eff} \left(|\vec{r}_p - \vec{r}_t + \vec{R}| \equiv r \right) d^3 r_p d^3 r_t, \quad (9)$$

obtained by using the well known double folding procedure [3] for the M3Y and the recently developed R3Y interaction potential, proposed in the Refs. [18, 19, 57], supplemented by zero-range pseudo-potential representing the single-nucleon exchange effects (EX). Adding Coulomb potential $V_C(R)$ ($= Z_p Z_t e^2 / R$) results in Nucleus-Nucleus interaction potential $V_T(R)$ [$= V_n(R) + V_C(R)$], used for calculating the fusion properties. As, we know the pairing play an important role in the nuclear bulk properties including the density distribution of open-shell nuclei, one has to consider the pairing correlation in their ground states [75]. In case of nuclei not too far from the β -stability line, one can use the constant gap BCS pairing approach reasonably good and simple to take care of pairing correlation [76]. The present analysis includes the intermediate mass nuclei around the β -stability, hence we have taken the relativistic mean field results with BCS treatment for pairing correlation [58, 60–62, 77, 78].

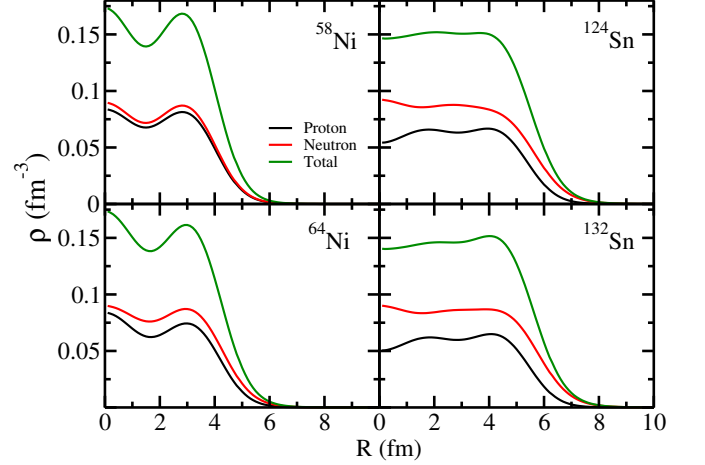


FIG. 1. (Color online) The RMF (NL3*) neutron, proton, and total radial density distribution for $^{58,64}\text{Ni}$, and $^{124,132}\text{Sn}$ nuclei. See text for details.

A. The Wong Formula

In terms of ℓ partial waves, the fusion cross-section for two nuclei, colliding with center-of-mass energy ($E_{c.m.}$), is given by [79]

$$\sigma(E_{c.m.}) = \frac{\pi}{k^2} \sum_{\ell} (2\ell + 1) P_{\ell}(E_{c.m.}), \quad (10)$$

with $k = \sqrt{\frac{2\mu E_{c.m.}}{\hbar^2}}$ and μ as the reduced mass. P_{ℓ} is the transmission coefficient for each ℓ which describes the penetration of barrier $V_T^{\ell}(R)$, given by

$$V_T^{\ell}(R) = V_n(R, A_i) + V_C(R, Z_i) + \frac{\hbar^2 \ell(\ell + 1)}{2\mu R^2}. \quad (11)$$

Using Hill-Wheeler [80, 81] approximation, the penetrability P_{ℓ} , in terms of its barrier height $V_B^{\ell}(E_{c.m.})$ and curvature $\hbar\omega_{\ell}(E_{c.m.})$, is

$$P_{\ell} = \left[1 + \exp \left(\frac{2\pi(V_B^{\ell}(E_{c.m.}) - E_{c.m.})}{\hbar\omega_{\ell}(E_{c.m.})} \right) \right]^{-1} \quad (12)$$

with $\hbar\omega_{\ell}$ evaluated at the barrier position $R = R_B^{\ell}$ corresponding to barrier height V_B^{ℓ} , given as

$$\hbar\omega_{\ell}(E_{c.m.}) = \hbar \left[|d^2 V_T^{\ell}(R) / dR^2|_{R=R_B^{\ell}} / \mu \right]^{1/2} \quad (13)$$

and, the R_B^{ℓ} obtained from the condition,

$$|dV_T^{\ell}(R) / dR|_{R=R_B^{\ell}} = 0.$$

Instead of solving Eq. (10) explicitly, which requires the complete ℓ -dependent potentials $V_T^{\ell}(R)$, Wong [79] carried out the ℓ -summation in Eq. (10) approximately under specific conditions:

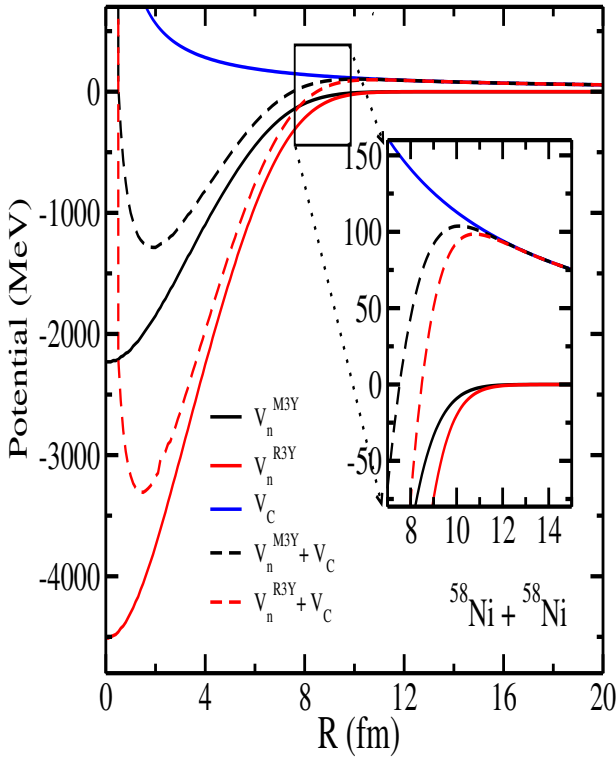


FIG. 2. (Color online) The total nucleus-nucleus optical potential $V(R)$ and the individual contributions [the nuclear $V_n(R)(M3Y+EX)$ and $V_n(R)(R3Y+EX)$ for NL3 parameter set, and the Coulomb $V_C(R)$ potential] as a function of radial separation R . The inset shows the barrier height and position in a magnified scale.

(i) $\hbar\omega_\ell \approx \hbar\omega_0$, and (ii) $V_B^\ell \approx V_B^0 + \frac{\hbar^2\ell(\ell+1)}{2\mu R_B^{0.2}}$, which means to assume $R_B^\ell \approx R_B^0$ also. In other words, both V_B^ℓ and $\hbar\omega_\ell$ are obtained for $\ell=0$ case. Using these approximations, and replacing the ℓ -summation in Eq. (10) by an integral, gives, on integration, the $\ell=0$ barrier-based Wong formula [79],

$$\sigma(E_{c.m.}) = \frac{R_B^{0.2}\hbar\omega_0}{2E_{c.m.}} \ln \left[1 + \exp \left(\frac{2\pi}{\hbar\omega_0} (E_{c.m.} - V_B^0) \right) \right]. \quad (14)$$

This is the simple formula used in the present work to calculate the fusion cross-section using the barrier characteristics such as V_B^0 , R_B^0 and $\hbar\omega_0$ within the barrier penetration model for spherical nuclei.

III. CALCULATION AND DISCUSSIONS

The RMF calculations furnish principally the fusion hindrance reaction phenomena using the self-consistent relativistic mean field formalism via Wong formula. In the first step, we calculate the nuclear structure properties such as the binding energy, quadrupole moment Q_{20} , the total density distribution $\rho(r_\perp, z)$ (i.e. the sum of

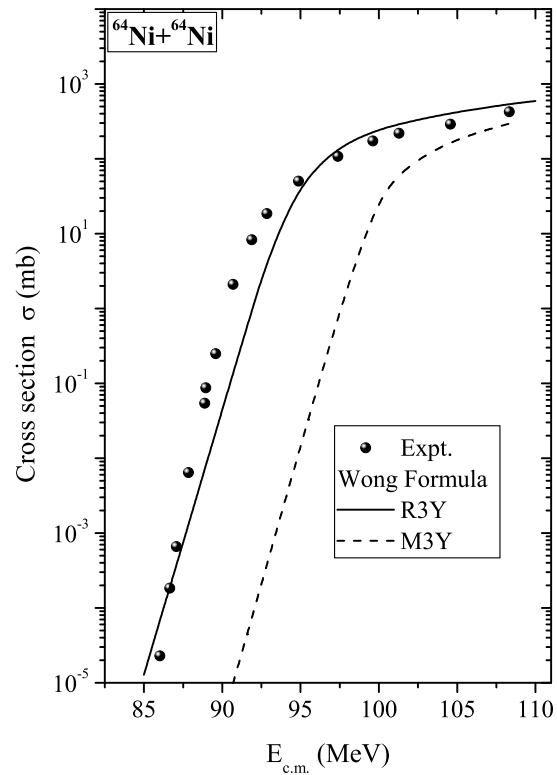


FIG. 3. Fusion-evaporation cross-section as a function of center-of-mass $E_{c.m.}$, calculated by using the Wong formula for R3Y (solid line) and M3Y (dashed line) NN -interactions, and compared with experimental data for $^{64}\text{Ni} + ^{64}\text{Ni}$ [30]. See the text for details.

the proton $\rho_p(r_\perp, z)$ and neutron $\rho_n(r_\perp, z)$ densities), the root-mean-square nuclear (neutron, proton and charge) radii and the single particle energy level for nucleons. Instead of concentrating on nuclear structure output profile for the NL3* force parameter, we use the monopole component of the densities for the target (t) and projectile (p) as the input for estimation of the optical nucleus-nucleus interaction potential using Eq. (9). The expression for the spin-independent proton and neutron mean-field densities from RMFT as,

$$\rho(\mathbf{R}) = \rho(r_\perp, z). \quad (15)$$

Here r_\perp and z are the cylindrical coordinates of the radial vector \mathbf{R} . The single particle densities are

$$\rho_i(\mathbf{R}) = \rho_i(r_\perp, z) = |\phi_i^+(r_\perp, z)|^2 + |\phi_i^-(r_\perp, z)|^2, \quad (16)$$

where, ϕ_i^\pm is the wave function, expanded into the eigen functions of an axially symmetric deformed harmonic oscillator potential in cylindrical co-ordinates. The normalization of the densities is given by,

$$\int \rho(\mathbf{R}) d\mathbf{R} = X, \quad (17)$$

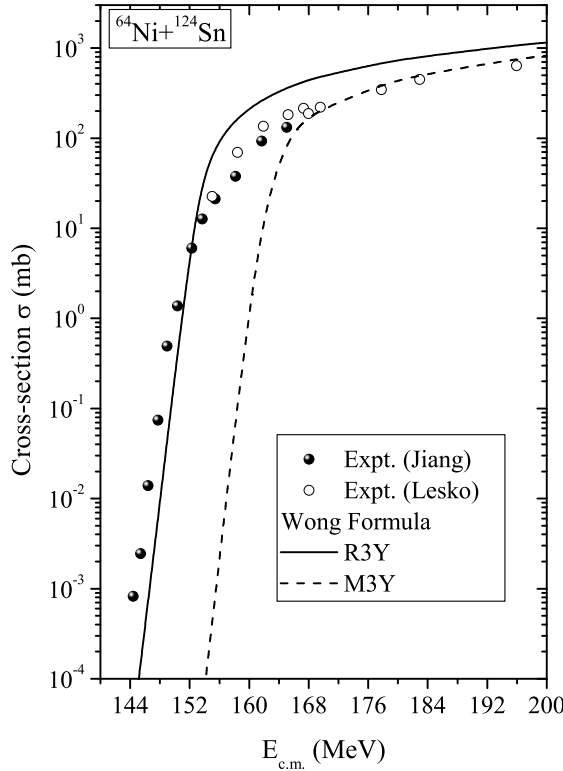


FIG. 4. Same as for Fig. 3, but for the reaction of $^{64}\text{Ni} + ^{124}\text{Sn}$. The experimental data is taken from Refs. [31–33]. See the text for details.

where $X = N, Z$ for neutron and proton number, respectively. Further, the multipole decomposition of the density can be written in terms of even values of the multipole index λ as,

$$\rho(r_{\perp}, z) = \sum_{\lambda} \rho_i(\mathbf{R}) P_{\lambda}(\cos\theta). \quad (18)$$

The monopole component of the density distribution of the expansion in the Eq. (18) are used for calculating the nucleus-nucleus optical potential. In Fig. 1, we have plotted the neutron (black solid line), proton (red solid line) and total density (green solid line) distribution for $^{58,64}\text{Ni}$ and $^{124,132}\text{Sn}$ obtained from the NL3* force parameter as a function of radius. From the figure, one can find that the central density a bit smaller in magnitude and enhanced a little towards the surface region in case of $^{124,132}\text{Sn}$ than that of $^{58,64}\text{Ni}$, which accepted to be the common feature in the heavy nucleus, play significant roles in the scattering studies [82].

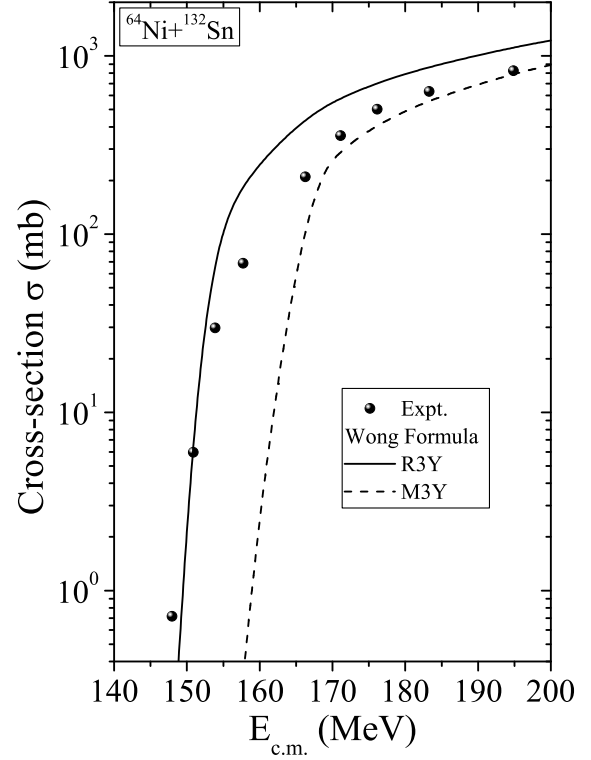


FIG. 5. Same as for Fig. 3, but for the reaction of $^{64}\text{Ni} + ^{132}\text{Sn}$. The experimental data is taken from Refs. [34, 35]. See the text for details.

A. Nucleus-Nucleus Optical Potential

The nuclear interaction potential $V_n(R)$ between the projectile (p) and target (t) nuclei is calculated using the well known double folding procedure in Eq. (9) [3, 18] from respective RMF matter densities ρ_p and ρ_t for M3Y and recently developed relativistic R3Y NN potential. The R3Y interaction is estimated for NL3* force parameter for present analysis [19, 60, 61], in which an effective Lagrangian is taken to describe the nucleons interaction through the effective mesons and electromagnetic fields. It is worth mentioning that the applicability of our newly introduced R3Y interaction potentials are used for the radioactivity studies of some highly unstable proton and/or neutron rich nuclei using preformed cluster decay model (PCM) of Gupta and co-workers [18–20]. The conservation of the angular momentum in the present analysis only limit to the ground state for estimate fusion characteristics of the constituent nuclei. To co-relate the theoretical calculation with the experimental fusion data, one need to adjust the spectroscopic factor by including the particle vibration coupling. Nevertheless, without this particle vibration coupling our present formalism simply

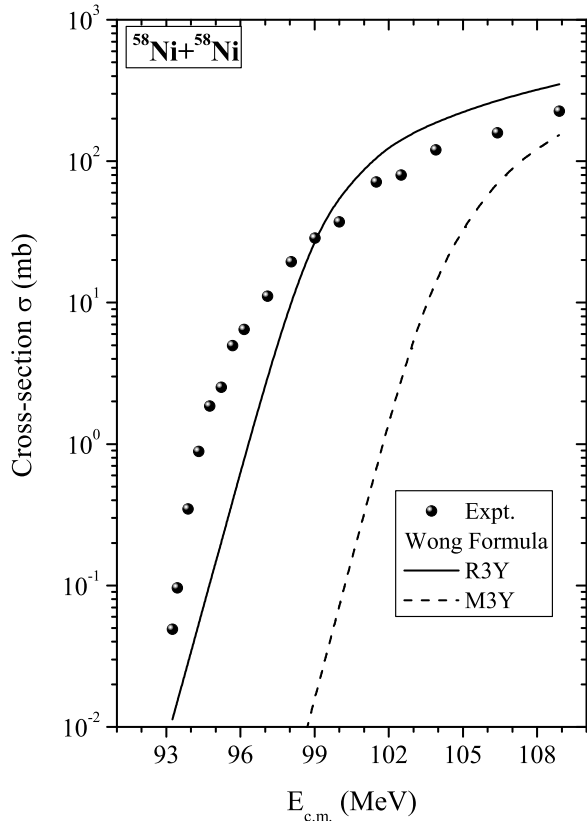


FIG. 6. Same as for Fig. 3, but for the reaction of $^{58}\text{Ni} + ^{58}\text{Ni}$. The experimental data is taken from Refs. [36]. See the text for details.

with the nonlinear $\sigma-$ mesons in Eq. (6), which is able to produce reasonable agreement with the experimental data [19]. Furthermore, these non-linear terms in the $\sigma-$ field plays an important role in the nuclear matter study and the detailed nuclear structure inherited by the density while calculating the proton and cluster decay properties (mostly a surface phenomenon) [61, 62].

The total interaction potentials $V_T(R) = V_n(R) + V_C(R)$ for the Ni-based reaction such as $^{64}\text{Ni} + ^{64}\text{Ni}$, $^{64}\text{Ni} + ^{124}\text{Sn}$, $^{64}\text{Ni} + ^{132}\text{Sn}$, $^{58}\text{Ni} + ^{58}\text{Ni}$, $^{58}\text{Ni} + ^{124}\text{Sn}$, and $^{58}\text{Ni} + ^{132}\text{Sn}$ systems are obtained for the M3Y+EX and R3Y+EX interactions for NL3* densities. As a representative case, the obtained results for total interaction potentials along with the Coulomb potential V_C and the nucleus-nucleus interactions without Coulomb for M3Y+EX and R3Y+EX interactions for $^{58}\text{Ni} + ^{58}\text{Ni}$ system is displayed in Fig. 2. From the figure, we note that the nature of the total $V_T(R)$ and the nuclear $V_n(R)$ potentials are similar for both the R3Y+EX and M3Y+EX NN -interactions (see Fig. 2). Quantitatively, both the nuclear potentials obtained from M3Y and R3Y differ significantly particularly in the central

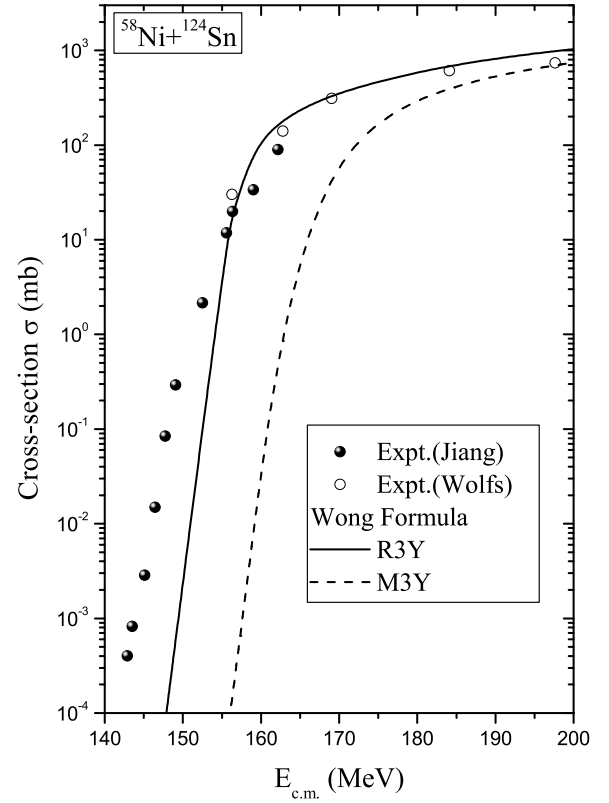


FIG. 7. Same as for Fig. 3, but for the reaction of $^{58}\text{Ni} + ^{124}\text{Sn}$. The experimental data is taken from Refs. [33, 37, 38]. See the text for details.

region and this difference reduced simultaneously with respect to the radial distance. Further, the height of the barrier for M3Y NN -interaction is a bit higher as compare to R3Y case (see the more clearly in the inset of Fig. 2). For example, the R3Y+EX is being more attractive by about 1 MeV with a barrier height lower by a few keV, compared to the M3Y+EX NN -interaction, as is illustrated in the inset of Fig. 2.

B. Fusion cross-sections

The barrier characteristics of the nuclear interaction potential i.e. barrier height, position and frequency from the total interaction potential are used in Wong formula [see Eq. (14)] for estimating the fusion reaction cross-section for the systems such as $^{64}\text{Ni} + ^{64}\text{Ni}$, $^{64}\text{Ni} + ^{124}\text{Sn}$, $^{64}\text{Ni} + ^{132}\text{Sn}$, $^{58}\text{Ni} + ^{58}\text{Ni}$, $^{58}\text{Ni} + ^{124}\text{Sn}$, and $^{58}\text{Ni} + ^{132}\text{Sn}$, known for fusion hindrance phenomena. Fig. 3 shows the comparison of fusion cross-section obtained for $^{64}\text{Ni} + ^{64}\text{Ni}$ around the Coulomb barrier with the experimental data [30]. The solid line shows the fusion cross-section using R3Y interaction and dashed line

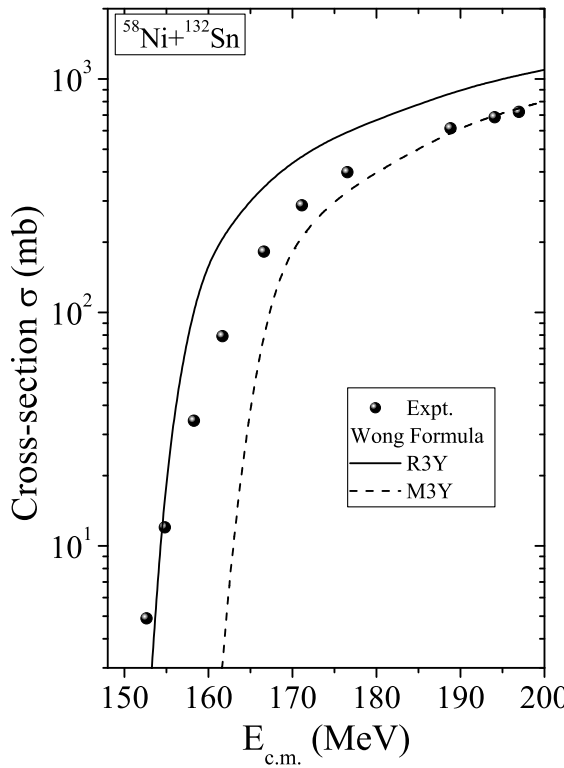


FIG. 8. Same as for Fig. 3, but for the reaction of $^{58}\text{Ni} + ^{132}\text{Sn}$. The experimental data is taken from Refs. [39]. See the text for details.

using M3Y potential within the Wong formula for NL3* densities. It is observed that R3Y performs relatively superior than M3Y interaction in comparison with the experimental data [30] below barrier energies. Motivated by this observation, the above said calculations are then pursued for $^{64}\text{Ni} + ^{124}\text{Sn}$ and $^{64}\text{Ni} + ^{132}\text{Sn}$ reactions as shown in Fig. 4, and Fig. 5, respectively. The experimental datas [31–35] are given for comparison. For the $^{64}\text{Ni} + ^{124}\text{Sn}$ reaction, the experimental datas [31–33] are available for near and/or below and other is above Coulomb barrier center of mass energies. In Figs. 4 and 5, the solid line is for R3Y and dashed for M3Y potential. The cross-section corresponding to R3Y are relatively close to the experimental data for energies below the Coulomb barrier whereas the M3Y fits the data only at above barrier energies. In other words, the nuclear interaction from R3Y potential explain the cross-section at comparatively lower energies. It is to be noted that the fusion cross-section corresponding to R3Y interaction is always larger as compare to that of M3Y potential. Furthermore a few similar calculations are done for another Ni-based reactions i.e. $^{58}\text{Ni} + ^{58}\text{Ni}$, $^{58}\text{Ni} + ^{124}\text{Sn}$ and $^{58}\text{Ni} + ^{132}\text{Sn}$ shown in Fig. 6, 7, and 8, respectively with

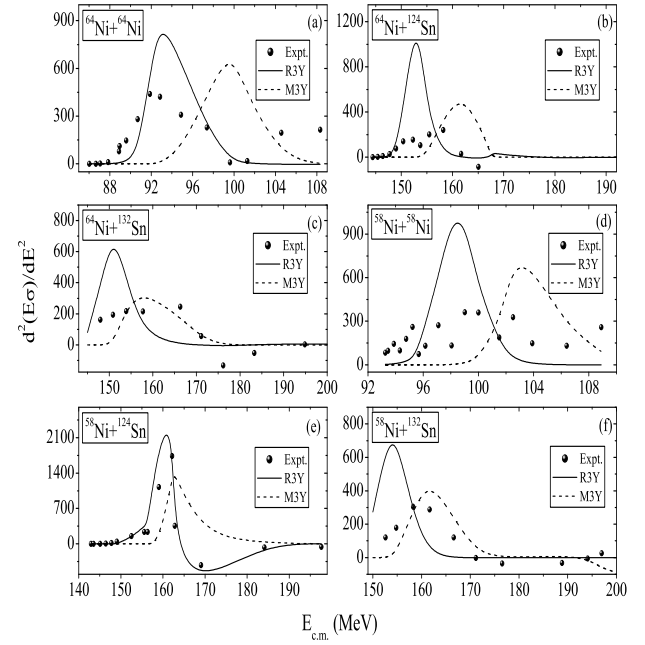


FIG. 9. The barrier distributions for the reactions (a) $^{64}\text{Ni} + ^{64}\text{Ni}$, (b) $^{64}\text{Ni} + ^{124}\text{Sn}$, (c) $^{64}\text{Ni} + ^{132}\text{Sn}$, (d) $^{58}\text{Ni} + ^{58}\text{Ni}$, (e) $^{58}\text{Ni} + ^{124}\text{Sn}$ and (f) $^{58}\text{Ni} + ^{132}\text{Sn}$ as a function of center-of-mass energy. The experimental datas are taken from the Refs. [30–39]. See the text for details.

the experimental datas [36–39]. It is clear from all these systems in Figs. 3, 4, 5, 6, 7, and 8 that the recently developed R3Y interaction within NL3* force parameter is proven to be relatively better choice than M3Y for considering the fusion reactions below the barrier at low energies. In other words, R3Y interaction allows the nuclei to relax, which reduces the barrier height and hence increases the fusion cross-section.

The transmission function is accomplished to obtain the fusion barrier distribution $\frac{d^2(E \cdot \sigma)}{dE^2}$ by differentiation with respect to center-of-mass energy. Classically, the transmission probability is a step function at an energy equal to the height of the fusion barrier. The Fermi function blur the step function into a smoother function, a parabolic barrier. The $\frac{d^2(E \cdot \sigma)}{dE^2}$ from fusion excitation functions are shown in Fig. 9 for the R3Y+EX (solid line) and M3Y+EX (dashed line) interactions. In the figure, we have shown the fusion barrier distribution for reduced cross-sections (a) $^{64}\text{Ni} + ^{64}\text{Ni}$, (b) $^{64}\text{Ni} + ^{124}\text{Sn}$, (c) $^{64}\text{Ni} + ^{132}\text{Sn}$, (d) $^{58}\text{Ni} + ^{58}\text{Ni}$, (e) $^{58}\text{Ni} + ^{124}\text{Sn}$ and (f) $^{58}\text{Ni} + ^{132}\text{Sn}$ along with the experimental data [30–39] for comparison. As expected, here we found the similar predictions as reaction cross-section, the obtained results from R3Y are relatively closer to the experimental data for energies below the Coulomb barrier whereas the M3Y

fits the data only above barrier energies. From the reaction cross-section and barrier distribution, one can conclude that the R3Y interaction produce relatively better than M3Y potential in comparison to experimental data. Hence, one can choice whole microscopic studies using the relativistic mean field density and the recently developed relativistic R3Y NN potential for fusion characteristic for above mentioned mass region to generate the nuclear potential within double folding procedure.

IV. SUMMARY AND CONCLUSIONS

We have investigated possible relationships between the nucleon-nucleon interaction potential and the fusion reaction cross-section for a few Ni-based systems, known for fusion hindrance phenomena. The fusion barrier distribution for the reduced fusion cross-section are also estimated from fusion excitation function for R3Y+EX and M3Y+EX interactions. We have considered six reaction systems such as $^{64}\text{Ni} + ^{64}\text{Ni}$, $^{64}\text{Ni} + ^{124}\text{Sn}$, $^{64}\text{Ni} + ^{132}\text{Sn}$, $^{58}\text{Ni} + ^{58}\text{Ni}$, $^{58}\text{Ni} + ^{124}\text{Sn}$ and $^{58}\text{Ni} + ^{132}\text{Sn}$ for present analysis. A microscopic approach based on an axial deformed relativistic mean field with recently developed NL3* force has been used along with the Wong formula to provide a transparent and analytic way to calculate the fusion cross-section by means of a convenient approach to the nucleus-nucleus optical potential. We have considered the well-known M3Y and the recently developed relativistic R3Y nucleon-nucleon interaction for

estimating the nuclear interaction potential. The NL3* densities for target and projectile are used for calculating the nuclear potential within double folding procedure for the study of fusion at low energies. It is worth mentioning that the quadrupole, odd multipole (octupole, etc.) shape degrees of freedom and/or the corresponding space reflection symmetry may provide some of these interesting issues and will throw more light on the fusion properties. We found that the R3Y interaction is proven to be better choice than M3Y for considered fusion reactions below the barrier energies in prediction of cross-section. Thus it can be inferred that R3Y interaction allows interacting nuclei to recline, which leads to lowering the barrier and hence increase the cross-section appreciably at the energies below the Coulomb barrier. The present analysis pursue a full microscopic studies by taking the R3Y potential along with the relativistic mean field densities within double folding procedure.

ACKNOWLEDGMENTS

This work has been supported by FAPESP Project Nos. 2014/26195-5 & 2017/05660-0, INCT-FNA Project No. 464898/2014-5, Seed Money Project of Thapar Institute of Engineering and Technology, Department of Science and Technology (DST), Govt. of India Project No. YSS/2015/000342 under Young Scientist Scheme, and by the CNPq - Brasil.

[1] K. A. Brueckner and K. M. Watson, Phys. Rev. **92**, 1023 (1953).
[2] J. W. Alcock and W. N. Cottingham, Nucl. Phys. B **41**, 141 (1972).
[3] G. R. Satchler and W. G. Love, Phys. Reports **55**, 183 (1979).
[4] R. V. Reid, Ann. Phys. (N.Y.) **50**, 411 (1968).
[5] W. N. Cottingham, M. Lacombe, B. Loiseau, J. M. Richard, and R. Vinh Mau, Phys. Rev. D **8**, 800 (1973).
[6] T. Hamada and I. D. Johnston, Nucl. Phys. **34**, 382 (1962).
[7] K. E. Lassila, M. H. Hull, H. M. Ruppel, F. A. McDonald and G. Breit, Phys. Rev. **126**, 881 (1962).
[8] B. D. Day, Phys. Rev. C **24**, 1203 (1981).
[9] V. G. J. Stoks, R. A. M. Klomp, C. P. F. Terheggen and J. J. de Swart, Phys. Rev. C **49**, 2950 (1994).
[10] H. Yukawa, Proc. Phys. Math. Soc. Jpn **17**, 48 (1935).
[11] E. Epelbaum, H.-W. Hammer and Ulf-G. Meiner, Rev. Mod. Phys. **81**, 1773 (2009).
[12] F. Gross, T. D. Cohen, E. Epelbaum and R. Machleidt, *Conference discussion of the nuclear force*, Few-Body Syst. **50**, 31 (2011).
[13] M. Garcon and J. W. Van Orden, Adv. Nucl. Phys. **26**, 293 (2001).
[14] S. Weinberg, Physica A **96**, 327 (1979).
[15] S. Weinberg, Phys. Lett. B **251**, 288 (1990).
[16] D. B. Kaplan, M. J. Savage and M. B. Wise, Phys. Lett. B **424**, 390 (1998).
[17] D. B. Kaplan, M. J. Savage and M. B. Wise, Nucl. Phys. B **534**, 329 (1998).
[18] B. B. Singh, M. Bhuyan, S. K. Patra, and R. K. Gupta, J. Phys. G: Nucl. Part. Phys. **39**, 025101 (2012).
[19] B. B. Sahu, S. K. Singh, M. Bhuyan, S. K. Biswal, and S. K. Patra, Phys. Rev. C **89**, 034614 (2014).
[20] M. Bhuyan, *Properties of finite nuclei using effective interaction*, LAP Lambert Academic Publishing, (2014).
[21] U. van Kolck, Prog. Part. Nucl. Phys. **43**, 337 (1999).
[22] E. Epelbaum, H.-W. Hammer, and Ulf-G. Meiner, Rev. Mod. Phys. **81**, 1773 (2009).
[23] A. Ekström, G. Baardsen, C. Forssén, G. Hagen, M. Hjorth-Jensen, G. R. Jansen, R. Machleidt, W. Nazarewicz, T. Papenbrock, J. Sarich and S. M. Wild, Phys. Rev. Lett. **110**, 192502 (2013).
[24] D. A. Goldberg, S. M. Smith, H.G. Pugh, P.G. Roos, and N.S. Waal, Phys. Rev. C **7**, 1938 (1973).
[25] H. G. Bohlen, M. R. Clover, G. Ingold, H. Lettau and W. von Oertzen, Z. Phys. A **308**, 121 (1882).
[26] E. Stiliarid, H. G. Bohlen, P. Frobrich, B. Gebauer, D. Kolbert, W. von Oertzen, M. Wilpert, and Th Wilpert, Phys. Lett. B **223**, 291 (1989).
[27] G. L. Zhang, H. Q. Zhang, Z. H. Liu, C. L. Zhang, C. J. Lin, F. Yang, G. P. An, H. M. Jia, Z. D. Wu, X. X. Xu, C. L. Bai, and N. Yu, High. Energy. Phys. Nucl. Phys.

31, 634 (2007).

[28] T. Dao Khoa, and G. R. Satchler, Nucl. Phys. A **668**, 3 (2000).

[29] A. Mukherjee *et al.*, Phys. Rev. C **66**, 034607 (2002).

[30] C. L. Jiang *et al.*, Phys. Rev. Lett. **93**, 012701 (2004).

[31] K. T. Lesko *et al.*, Phys. Rev. Lett. **55**, 803 (1985).

[32] K. T. Lesko *et al.*, Phys. Rev. C **34**, 2155 (1986).

[33] C. L. Jiang *et al.*, Phys. Rev. C **91**, 044602 (2015).

[34] J. F. Liang *et al.*, Phys. Rev. C **75**, 054607 (2007).

[35] J. F. Liang, D. Shapira, C. J. Gross, R. L. Varner, J. R. Beene, P. E. Mueller, and D. W. Stracener, Phys. Rev. C **78**, 047601 (2008).

[36] M. Beckerman *et al.*, Phys. Rev. C **23**, 1581 (1981).

[37] F. L. H. Wolfs, W. Henning, K. E. Rehm, and J. P. Schiffer, Phys. Lett. B **196**, 113 (1987).

[38] F. L. H. Wolfs, Phys. Rev. C **36**, 1379 (1987).

[39] Z. Kohley *et al.*, Phys. Rev. Lett. **107**, 202701 (2011).

[40] R. Vandenbosch, Annu. Rev. Nucl. Part. Sci. **42**, 447 (1992).

[41] A. B. Balantekin and N. Takigawa, Rev. Mod. Phys. **70**, 77 (1998).

[42] N. Rowley, G. R. Satchler, and P. H. Stelson, Phys. Lett. B **254**, 25 (1991).

[43] C. Vaz *et al.*, Phys. Rep. **69**, 373 (1981).

[44] R. G. Stokstad *et al.*, Phys. Rev. Lett. **41**, 465 (1978).

[45] R. G. Stokstad *et al.*, Phys. Rev. C **21**, 2427 (1980).

[46] C. L. Jiang *et al.*, Phys. Rev. Lett. **89**, 052701 (2002).

[47] C. J. Lin *et al.*, Phys. Rev. Lett. **91**, 229201 (2003).

[48] C. L. Jiang, B. B. Back, H. Esbensen, R. V. F. Janssens, and K. E. Rehm, Phys. Rev. C **73**, 014613 (2006).

[49] C. L. Jiang, B. B. Back, R. V. F. Janssens, and K. E. Rehm, Phys. Rev. C **75**, 057604 (2007).

[50] K. Hagino *et al.*, Phys. Rev. C **67**, 054603 (2003).

[51] C. L. Jiang, K. E. Rehm, B. B. Back, H. Esbensen, R. V. F. Janssens, A. M. Stefanini, and G. Montagnoli, Phys. Rev. C **89**, 051603(R) (2014).

[52] M. Dasgupta and D. J. Hinde, Annu. Rev. Nucl. Part. Sci. **48**, 401 (1998).

[53] J. Boguta and A. R. Bodmer, Nucl. Phys. A **292**, 413 (1977).

[54] B. D. Serot and J. D. Walecka, in *Advances in Nuclear Physics*, edited by J. W. Negele and Erich Vogt *Plenum Press, New York*, Vol. **16**, p. 1 (1986).

[55] W. Pannert, P. Ring, and J. Boguta, Phys. Rev. Lett., **59**, 2420, (1986).

[56] S. K. Singh, M. Bhuyan, P. K. Panda and S. K. Patra, J. Phys. G: Nucl. Part. Phys. **40**, 085104 (2013).

[57] S. K. Singh, S. K. Biswal, M. Bhuyan and S. K. Patra, J. Phys. G: Nucl. Part. Phys. **41**, 055201 (2014).

[58] S. K. Patra, M. Bhuyan, M. S. Mehta and R. K. Gupta, Phys. Rev. C **80**, 034312 (2009).

[59] M. Bhuyan, S. K. Patra, and R. K. Gupta, Phys. Rev. C **84**, 014317 (2011).

[60] M. Bhuyan, Phys. Rev. C **92**, 034323 (2015).

[61] M. Bhuyan, B. V. Carlson, S. K. Patra, and Shan-Gui Zhou, Phys. Rev. C **97**, 024322 (2018).

[62] M. Bhuyan, Phys. Atm. Nucl. **81**, 15 (2018).

[63] G. A. Lalazissis, S. Raman and P. Ring, Atm. Data. Nucl. Data. Table. **71**, 1 (1999).

[64] P. -G. Reinhard, Rep. Prog. Phys. **52**, 439 (1989).

[65] P. Ring, Prog. Part. Nucl. Phys. **37**, 193 (1996).

[66] D. Vretenar, A. V. Afanasjev, G. A. Lalazissis, and P. Ring, Phys. Rep. **409**, 101 (2005).

[67] J. Meng, H. Toki, S. G. Zhou, S. Q. Zhang, W. H. Long, and L. S. Geng, Prog. Part. Nucl. Phys. **57**, 470 (2006).

[68] N. Paar, D. Vretenar, and G. Colo, Rep. Prog. Phys. **70**, 691 (2007).

[69] T. Nikšić, D. Vretenar, and P. Ring, Prog. Part. Nucl. Phys. **66**, 519 (2011).

[70] Xian-Feng Zhao, and Huan-Yu Jia, Phys. Rev. C **85**, 065806 (2012).

[71] G. A. Lalazissis, S. Karatzikos, R. Fossoin, D. Pena Arteaga, A. V. Afanasjev, P. Ring, Phys. Lett. B **671**, 36 (2009).

[72] M. Bender, P.-H. Heenen, and P.-G. Reinhard, Rev. Mod. Phys. **75**, 121 (2003).

[73] L.I. Schiff, Phys. Rev. **84**, 1 (1951).

[74] D. Vautherin and M. Veneroni, Phys. Lett. B **29**, 203 (1969).

[75] S. Karatzikos, A. V. Afanasjev, G. A. Lalazissis, P. Ring, Phys. Lett. B **689**, 72 (2010).

[76] J. Dobaczewski, H. Flocard, J. Treiner, Nucl. Phys. A **422**, 103 (1984).

[77] D. G. Madland and J. R. Nix, Nucl. Phys. A **476**, 1 (1981).

[78] P. Möller and J.R. Nix, At. Data and Nucl. Data Tables **39**, 213 (1988).

[79] C. Y. Wong, Phys. Rev. Lett. **31**, 766 (1973).

[80] D. L. Hill and J. A. Wheeler, Phys. Rev. **89**, 1102 (1953).

[81] T. D. Thomas, Phys. Rev. **116**, 703 (1959).

[82] M. Bhuyan, R. N. Panda, T. R. Routray and S. K. Patra, Phys. Rev. C **82**, 064602 (2010).